# Electronic Supplementary Information

## CoP and $Ni_2P$ implanted in hollow porous N-doped carbon polyhedron for pH universal hydrogen evolution reaction and alkaline overall water splitting

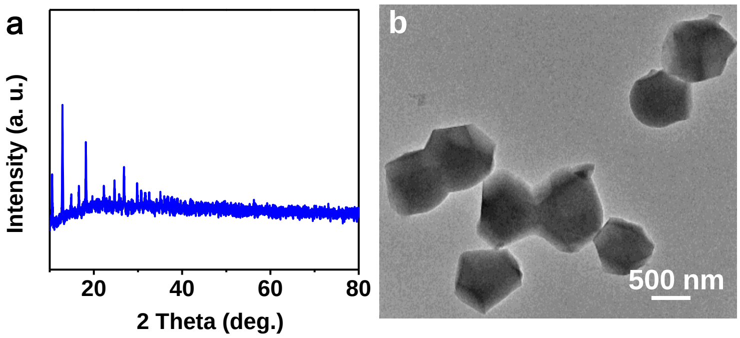


**Fig. S1** (a) XRD and (b) TEM image of ZIF-67

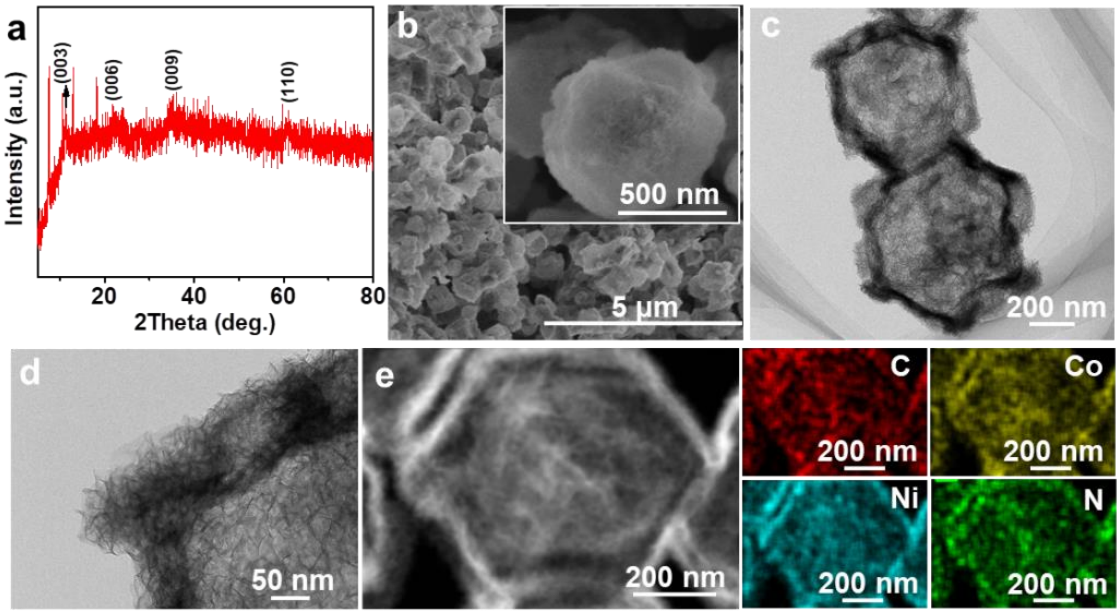


**Fig. S2** (a) XRD patterns, (b) SEM image, (c) low magnification and (d) high magnification TEM image and (e) HAADF-STEM image and corresponding elemental mapping of Co/Ni-LDH@ZIF-67.

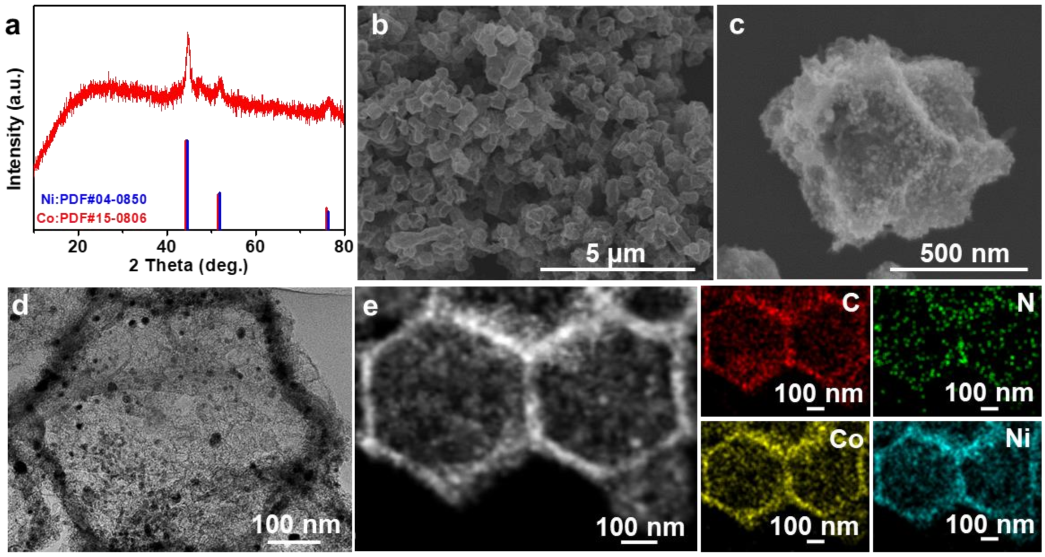


**Fig. S3** (a) XRD patterns, (b) low magnification and (c) high magnification SEM images, (d) TEM image, (e) HAADF-STEM image and corresponding EDS elemental mapping of the as-synthesized Co,Ni@HPNCP.

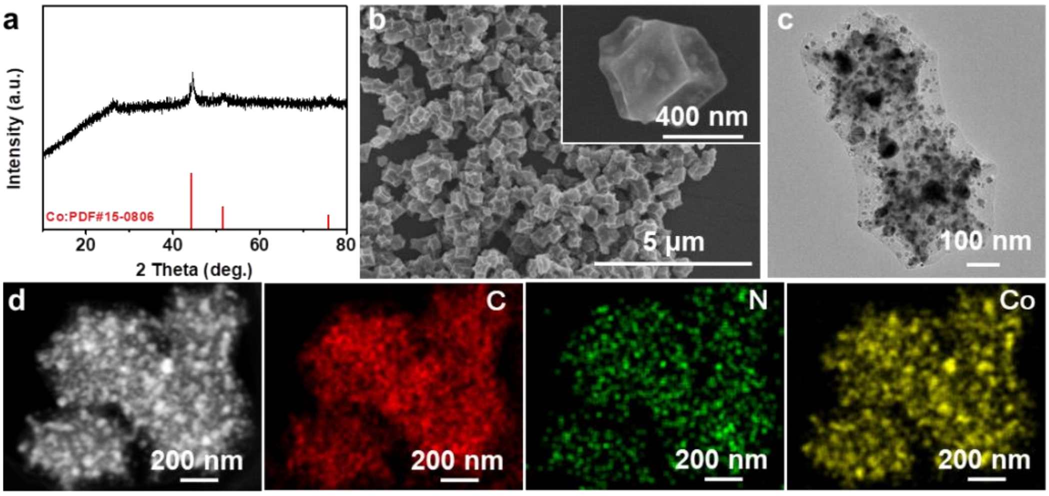


**Fig. S4** (a) XRD patterns, (b) SEM image, (c) TEM image, (d) HAADF-STEM image and corresponding EDS elemental mapping of the as-synthesized Co@NCP. Inset in (b) is magnified SEM image.

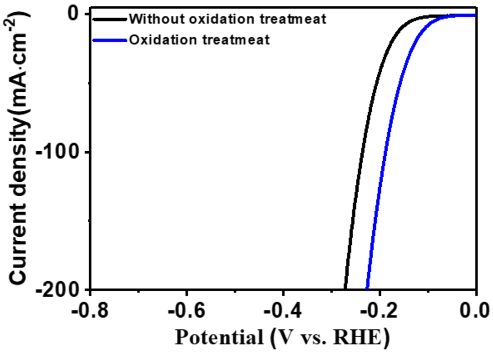


**Fig. S5** HER LSV curves of CoP/$Ni_2P$@HPNCP fabricated by phosphorization of Co/Ni@HPNCP with and without oxidation treatment in air.

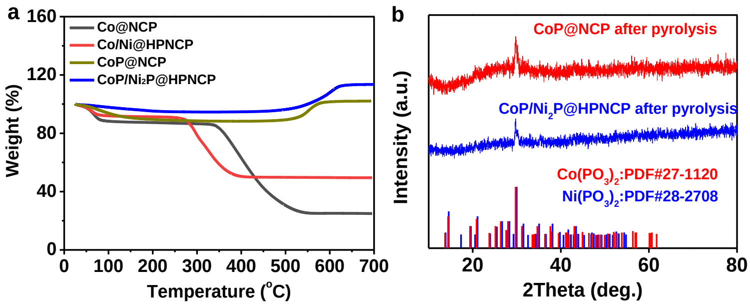


**Fig. S6** (a) TGA curves of CoP/$Ni_2P$@HPNCP, CoP@NCP, Co/Ni@HPNCP and Co@NCP in air, (b) XRD patterns of the residue after pyrolysis of CoP/$Ni_2P$@HPNCP and CoP@NCP.

The final residue (114.3 wt%) is $Co(PO_3)_2$ and $Ni(PO_3)_2$ based on TGA and XRD. Therefore, the relatively content of CoP and $Ni_2P$ in CoP/$Ni_2P$@HPNCP can be calculated by following equation:

$$(X/M(CoP)) \times M(Co(PO_3)_2)+(Y/M(Ni_2P)) \times 2 \times M(Ni(PO_3)_2)=1.143$$

where, M(CoP), M($Co(PO_3)_2$), M($Ni_2P$) and M($Ni(PO_3)_2$) is the molar mass of CoP, $Co(PO_3)_2$, $Ni_2P$ and ($Ni(PO_3)_2$. Because the ratio of Ni with Co is 1:5 based on ICP-MS measurement results,

$$(X/M(CoP)): (2Y/M(Ni_2P))=5:1$$

Therefore, the value of X and Y is 0.3953 and 0.0653, respectively. Consequently, the relative content of phosphide is 46.06 %.

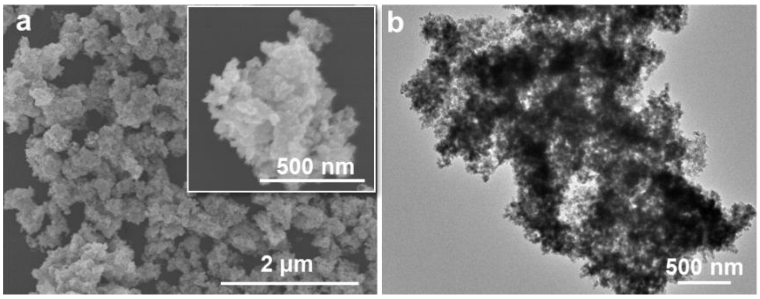


**Fig.** S7 (a) SEM and (b) TEM image of CoP@NCP.

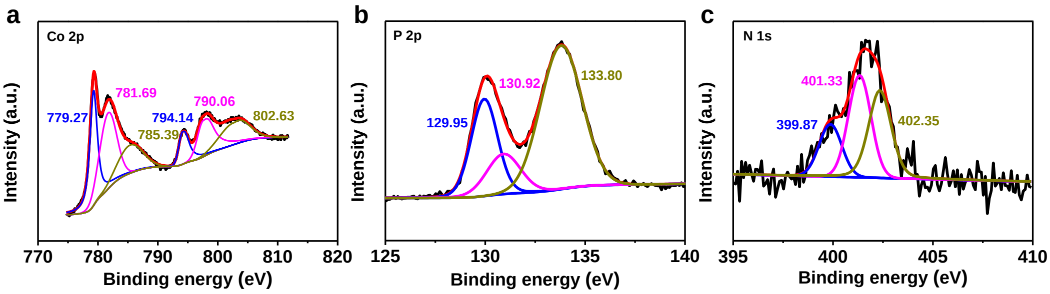


**Fig. S8** XPS high-resolution spectra of CoP@NCP: (a) Co 2p, (b) P 2p and (c) N 1s.

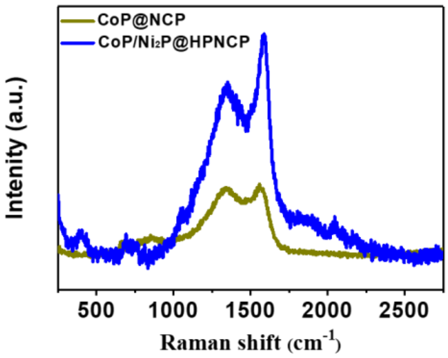


**Fig. S9** Raman spectra of $CoP/Ni_2P$@HPNCP and CoP@NCP.

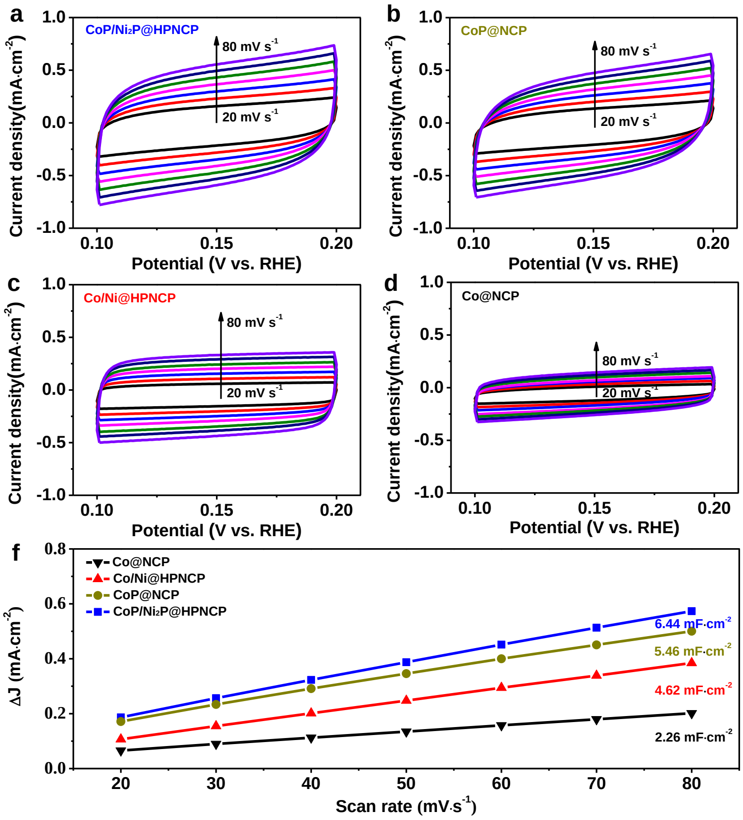


**Fig. S10** CV curves of (a)CoP/$Ni_2P$@HPNCP, (b) CoP@NCP, (c) Co/Ni@HPNCP and (d) Co@NCP in the non-faradaic capacitance from 0.10 V to 0.20 V vs. RHE at scan rate of 20, 30, 40, 50, 60, 70 and 80 mV $s^{-1}$ in 1.0 M KOH, (f) calculated $C_{dl}$ for CoP/$Ni_2P$@HPNCP, CoP@NCP, Co/Ni@HPNCP and Co@NCP.

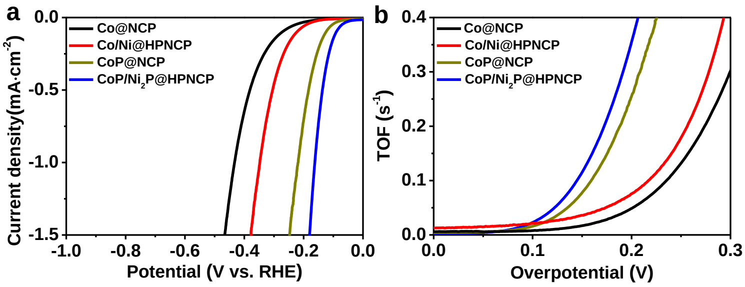


**Fig. S11** (a) Specific activity and (b) TOF of CoP/$Ni_2P$@HPNCP, CoP@NCP, Co/Ni@HPNCP and Co@NCP in 1.0 KOH.

The specific activity was calculated by normalizing the $C_{dl}$ to a standard specific capacitance (40 μF $cm^{-2}$).[1]Turnover frequency (TOF) can be obtained from the equation: TOF = (J × A)/ (z × F ×n), Where J is the current density at specific overpotential (mA $cm^{-2}$), A presents geometric area of the samples ($cm^{-2}$), F is faraday constant (96485 C $mol^{-1}$) and n represents the total moles number of all active metal sites, Z is the electron number transferred to product one molecule gas. For HER, N is 2, for OER, N is 4. [2-3]

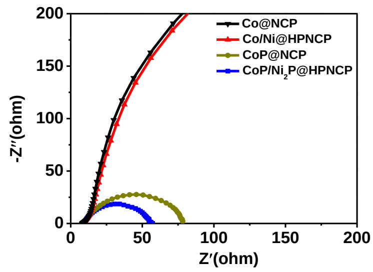


**Fig. S12** EIS of CoP/$Ni_2P$@HPNCP, CoP@NCP, Co/Ni@HPNCP and Co@NCP measured in 1.0 KOH.

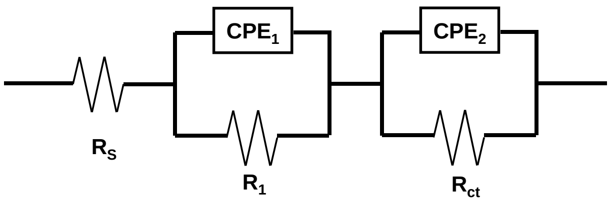


**Fig. S13** The equivalent circuit model of EIS analysis of all samples.

The equivalent circuit constitutes by a parallel combination of ($R_{ct}$, $CPE_1$) and ($R_2$, $CPE_2$) element in series with $R_s$. The CPE is regarded as the double layer capacitor from the catalyst/support and catalyst solution. $R_s$, $R_{ct}$ and $R_1$ is uncompensated solution resistance, charge transfer resistance and the contact resistance between the catalyst material and the others resistance, respectively.

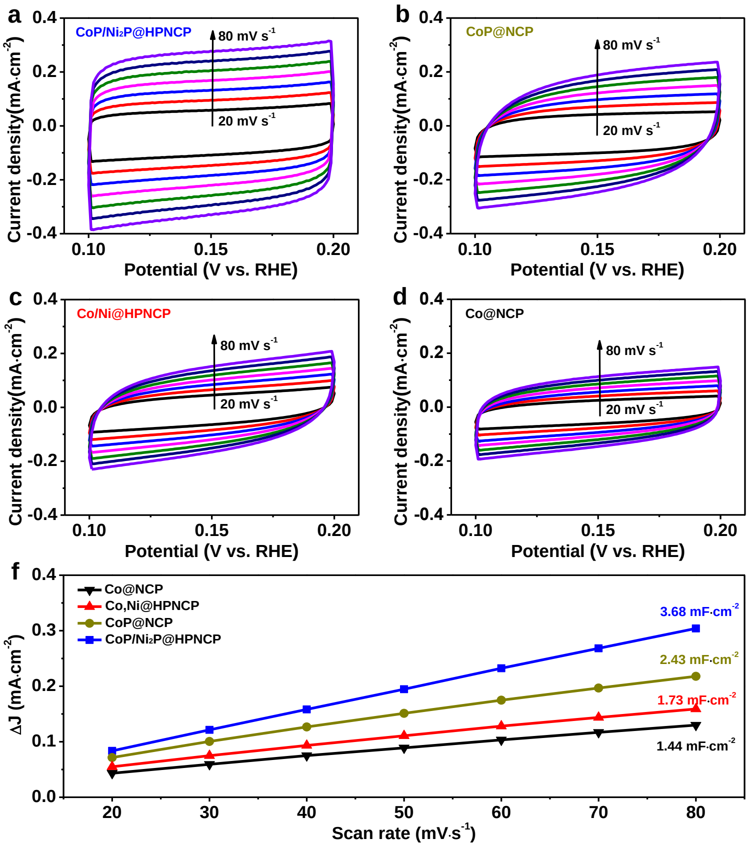


**Fig. S14** CV curves of (a)CoP/$Ni_2P$@HPNCP, (b) CoP@NCP, (c) Co/Ni@HPNCP and (d) Co@NCP in the non-faradaic capacitance from 0.10 V to 0.20 V vs. RHE at scan rate of 20, 30, 40, 50, 60, 70 and 80 mV $s^{-1}$ in 0.5 M $H_2SO_4$, (f) calculated $C_{dl}$ for CoP/$Ni_2P$@HPNCP, CoP@NCP, Co/Ni@HPNCP and Co@NCP.

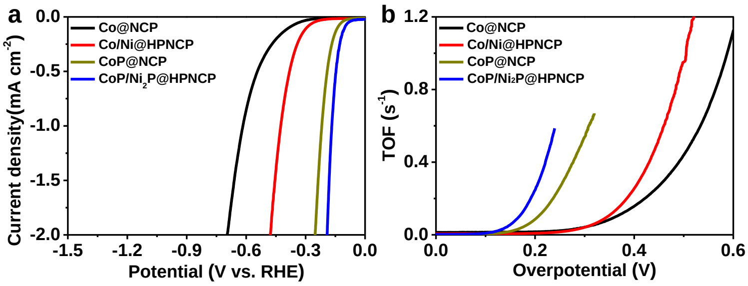


**Fig. S15** (a) Specific activity and (b) TOF of CoP/$Ni_2P$@HPNCP, CoP@NCP, Co/Ni@HPNCP and Co@NCP in 0.5 $H_2SO_4$.

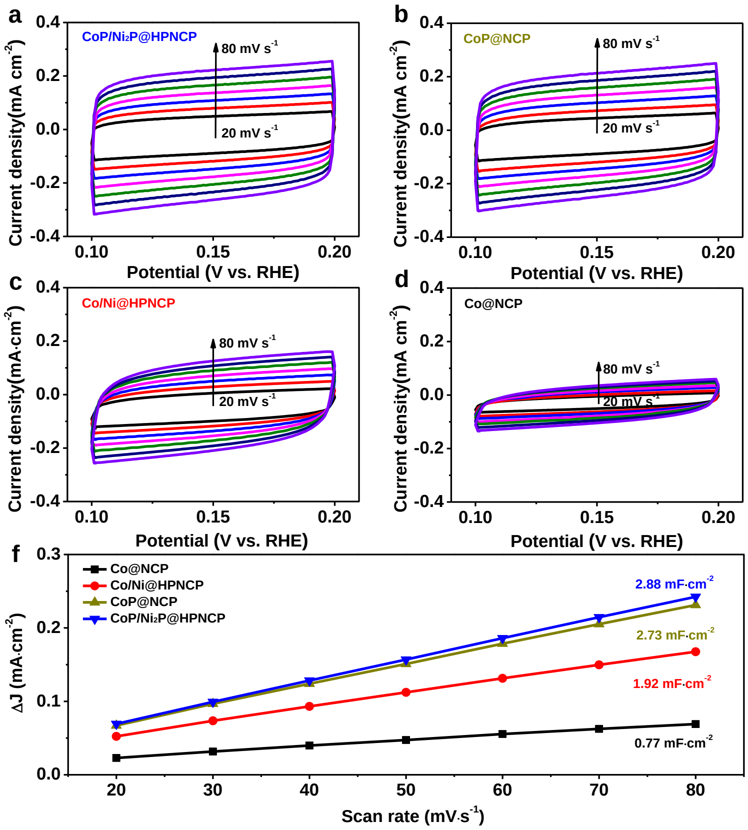


**Fig. S16** CV curves of (a)CoP/$Ni_2P$@HPNCP, (b) CoP@NCP, (c) Co/Ni@HPNCP and (d) Co@NCP in the non-faradaic capacitance from 0.10 V to 0.20 V vs. RHE at scan rate of 20, 30, 40, 50, 60, 70 and 80 mV $s^{-1}$ in 1.0 M PBS, (f) calculated $C_{dl}$ for CoP/$Ni_2P$@HPNCP, CoP@NCP, Co/Ni@HPNCP and Co@NCP.

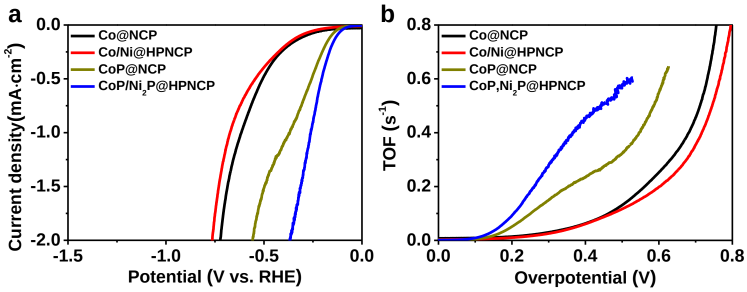


**Fig. S17** (a) Specific activity and (b) TOF of CoP/$Ni_2P$@HPNCP, CoP@NCP, Co/Ni@HPNCP and Co@NCP in 1.0 M PBS.

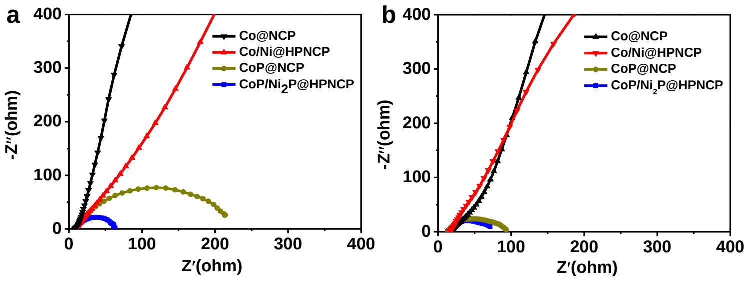


**Fig. S18** EIS of CoP/$Ni_2P$@HPNCP, CoP@NCP, Co/Ni@HPNCP and Co@NCP measured in (a) 0.5 $H_2SO_4$ and (b) 1.0 M PBS.

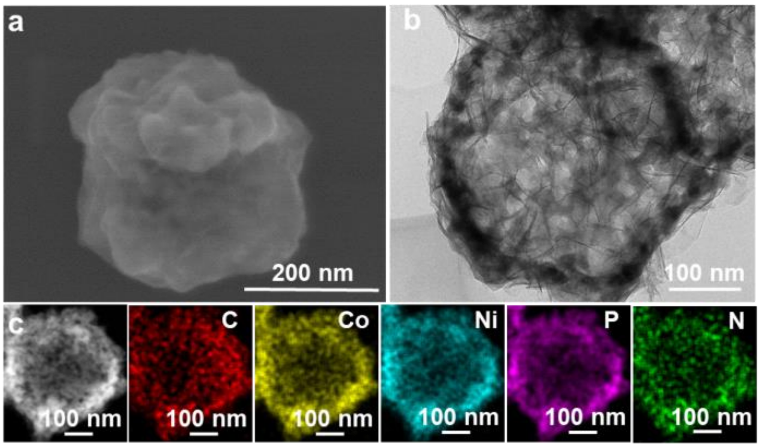


**Fig. S19** (a) SEM image, (b) TEM image, (c) HAADF-STEM image and corresponding EDS elemental mapping of CoP/$Ni_2P$@HPNCP after long-term test in 1.0 M KOH.

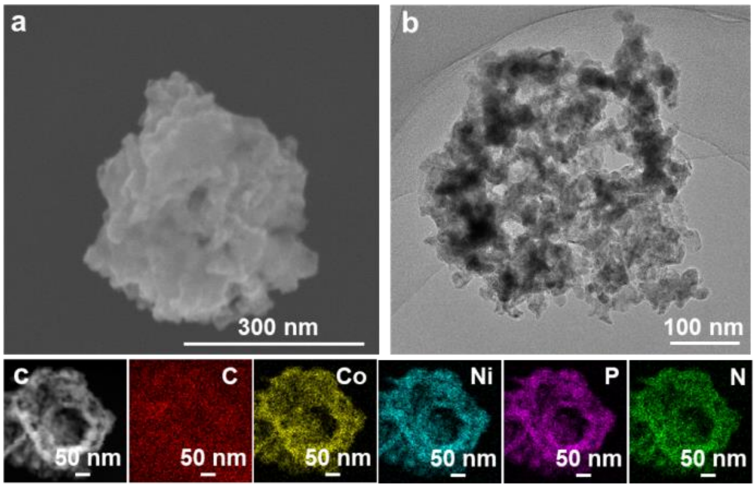


**Fig. S20** (a) SEM image, (b) TEM image, (c) HAADF-STEM image and corresponding EDS elemental mapping of CoP/$Ni_2P$@HPNCP after long-term test in 0.5 M $H_2SO_4$.

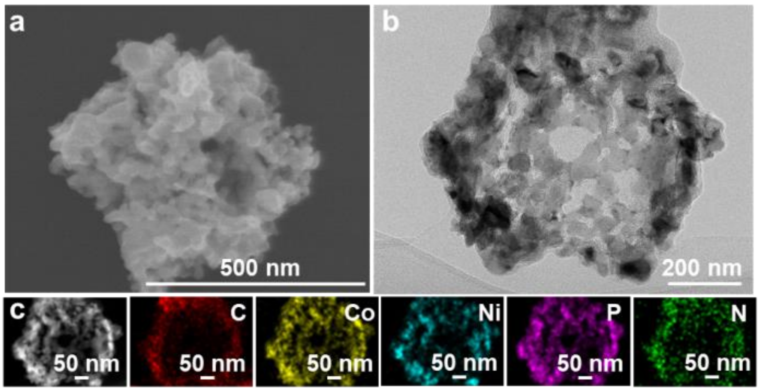


**Fig. S21** (a) SEM image, (b) TEM image, (c) HAADF-STEM and corresponding EDS elemental mapping of CoP/$Ni_2P$@HPNCP after long-term test in 1.0 M PBS.

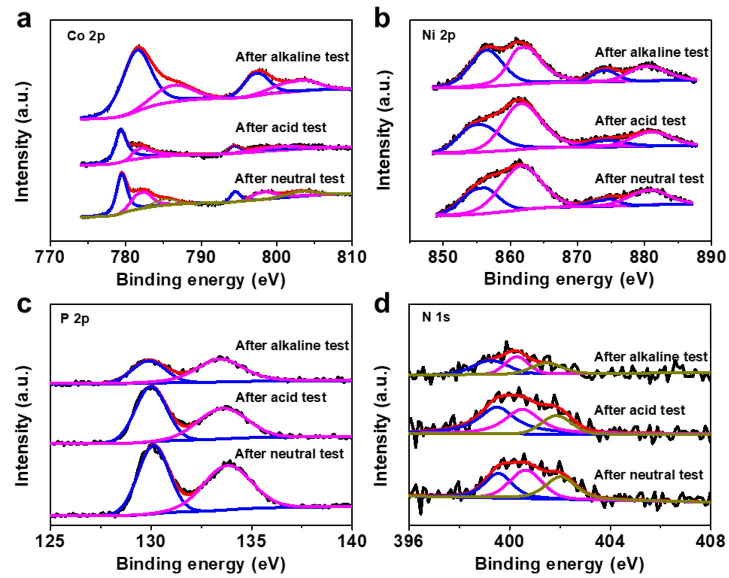


**Fig. S22** XPS high-resolution spectrua of CoP/$Ni_2P$@HPNCP after long-term HER test (a) Co 2p, (b) Ni 2P, (c) P 2p and (d) N 1s.

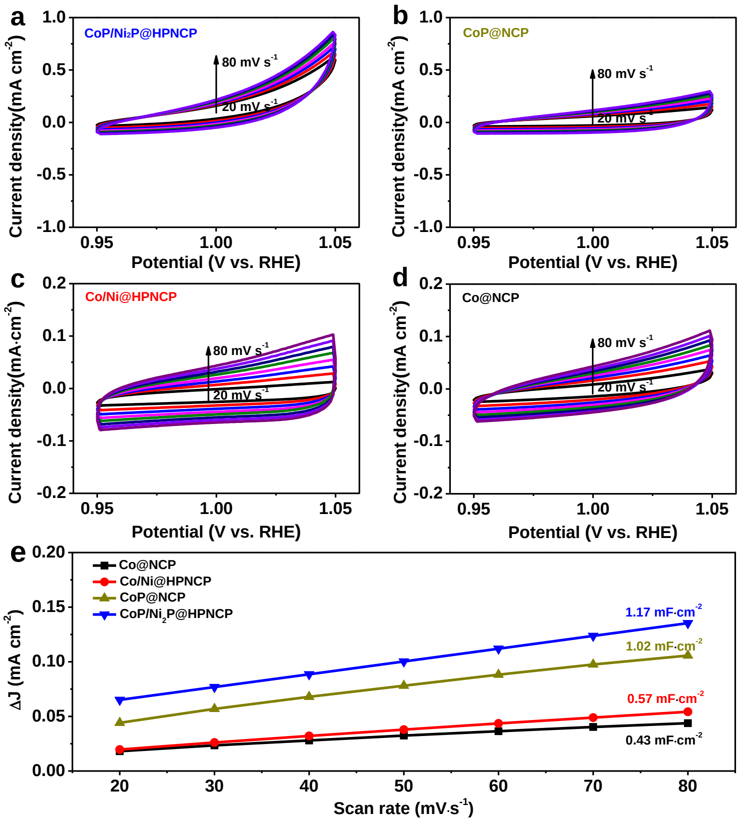


**Fig. S23** CV curves of (a)CoP/$Ni_2P$@HPNCP, (b) CoP@NCP, (c) Co/Ni@HPNCP and (d) Co@NCP in the non-faradaic capacitance from 0.95 V to 1.05 V vs. RHE at scan rate of 20, 30, 40, 50, 60, 70 and 80 mV $s^{-1}$ in 1.0 M KOH, (f) calculated $C_{dl}$ for CoP/$Ni_2P$@HPNCP, CoP@NCP, Co/Ni@HPNCP and Co@NCP.

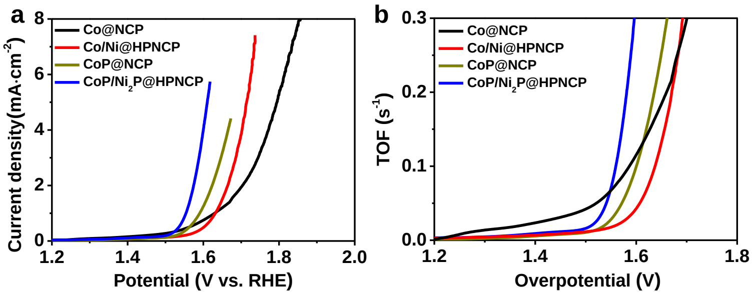


**Fig. S24** (a) Specific activity and (b) TOF of CoP/$Ni_2P$@HPNCP, CoP@NCP, Co/Ni@HPNCP and Co@NCP in 1.0 M KOH.

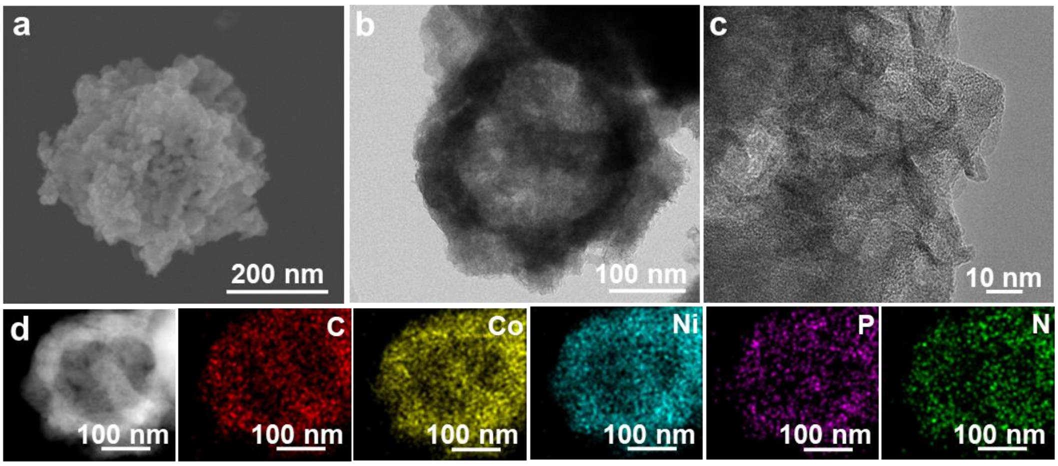


**Fig. S25** (a) SEM image, (b) TEM image, (c) HRTEM, (d) HAADF-STEM and corresponding EDS elemental mapping of CoP/$Ni_2P$@HPNCP after OER test.

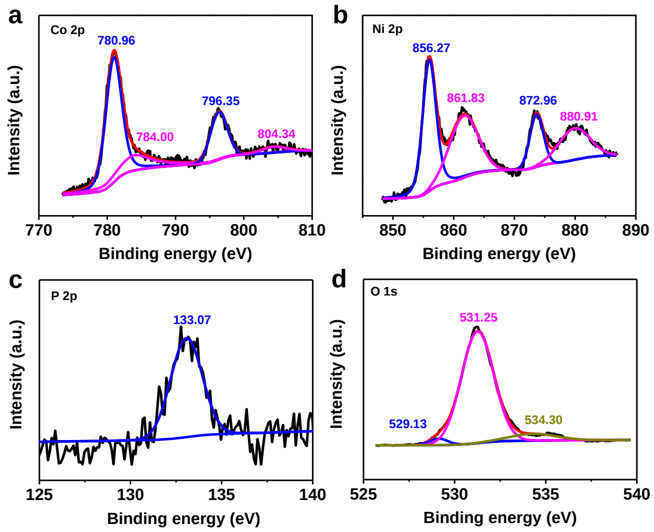


**Fig. S26** XPS high-resolution spectra of CoP/$Ni_2P$@HPNCP after OER test: (a) Co 2p, (b) Ni 2p, (c) P 2p and (d) O 1s.

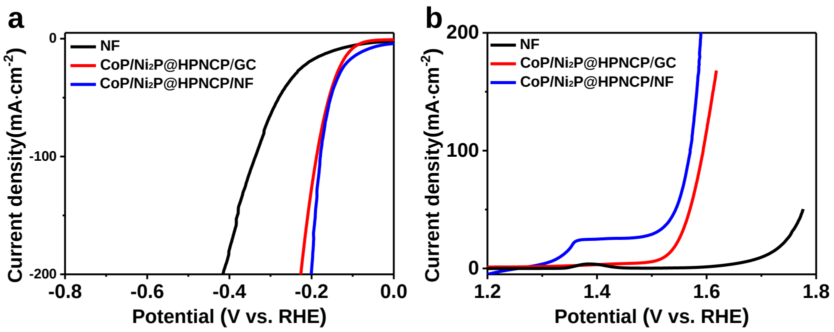


**Fig.** S27 (a) HER and (b) OER LSV curves of CoP/$Ni_2P$@HPNCP deposited on Ni foam and glass carbon electrode surface.

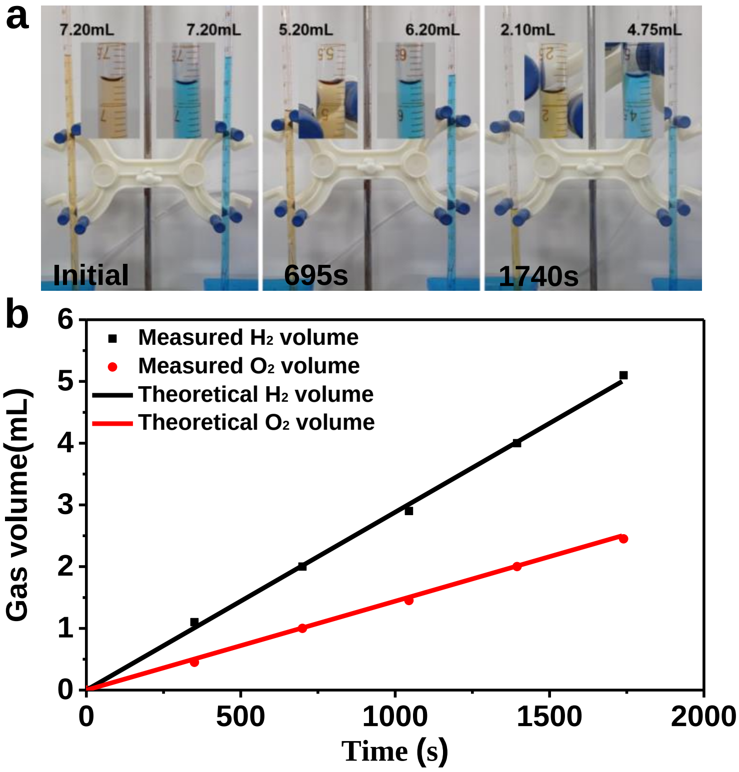


**Fig. S28** (a)The digital photo of $H_2$ and $O_2$ volume at different test time, (b) Volume of $H_2$ and $O_2$ as a function time at 0.025 A.

The theoretical volume of $H_2$ or $O_2$ during overall water splitting can be calculated by following equation

$$V=\frac{i\times t\times 22.4}{n\times F}$$

where, V is volume of $H_2$ or $O_2$ (L), n is the electron number transferred to product one molecule gas, F presents the faraday constant (96485 C mol$^{-1}$). i is applied current (A), t represents test time (s). In our experiment, i is 0.025 A.

**Table S1** Comparison of HER, OER and overall water splitting of CoP/$Ni_2P$@HPNCP with other reported phosphide-based bifunctional electrocatalysts in 1.0 M KOH.

| Catalysts | Overpotential at 10 mA $cm^{-2}$ (mV) | | Tafel slope (mV $dec^{-1}$) | | Electrolytic cell voltage at 10 mA $cm^{-2}$ (V) | Reference |
|---|---|---|---|---|---|---|
| | HER | OER | HER | OER | | |
| CoP/$Ni_2P$@HPNCP | 106 | 294 | 65.9 | 65.5 | 1.59 | This work |
| CoP/NCNHP | 115 | 310 | 66 | 70 | 1.64 | 4 |
| CoxP/N-doped C | 187 | 380 | 58.5 | 68.1 | 1.71 | 5 |
| CoP/EEBP | 118 | 315 | 79 | 75 | 1.666 | 6 |
| $Co_2P$/CoNPC | 208 | 326 | 72.6 | 83.9 | 1.64 | 7 |
| $Ni_2P$/NF | 116 | 290 (50) | 68 | 75 | 1.63 | 8 |
| NiCoFeP/C | 149 | 270 | 89 | 65 | 1.60 | 9 |
| $FeP_2$–$NiP_2$@PC | 179 | 248 | 65 | 54 | 1.70 | 10 |
| NiCoP@$Cu_3P$ | 54 | 309 | 72 | 42 | - | 11 |
| FeNi-LDH/CoP/CC | 138.6 (20) | 231 (20) | 56.1 | 33.5 | 1.617 | 12 |
| FeCo/$Co_2P$@NPCF | 260 | 330 | 120 | 61 | - | 13 |
| CoP/$Ni_2P$ | 200 | 300 | 103 | 60 | 1.60 | 14 |
| $Fe_{0.29}Co_{0.71}P$/NF | 74 | 251 (50) | 53.6 | 37.8 | 1.59 | 15 |

**Table S2** EIS fitting parameters from equivalent circuits of all samples during HER process in 1.0 M KOH.

| **Samples** | **$R_S$ /Ω** | **$CPE_1$ / S $s^{-n}$** | **$n_1$/ 0<n<1** | **$R_1$ / Ω** | **$CPE_2$ / S $s^{-n}$** | **$n_2$/ 0<n<1** | **$R_{ct}$ /Ω** |
|---|---|---|---|---|---|---|---|
| CoP/$Ni_2$P@HPNCP | 8.196 | 3.759 E-002 | 0.80 | 1.886 | 3.416 E-004 | 0.87 | 45.54 |
| CoP@NCP | 8.226 | 1.801 E-002 | 0.38 | 0.598 | 7.563 E-004 | 0.88 | 64.81 |
| Co/Ni@HPNCP | 7.739 | 9.394 E-004 | 0.39 | 0.465 | 1.465 E-002 | 0.44 | 710.5 |
| Co@NCP | 8.230 | 1.003 E-003 | 0.82 | 0.592 | 2.670 E-003 | 0.65 | 849.0 |

**Table S3** Comparison of HER of CoP/$Ni_2$P@HPNCP with other reported phosphide-based bifunctional electrocatalysts in 0.5 M $H_2SO_4$.

| **Catalysts** | **Overpotential at 10 mA $cm^{-2}$ (mV)** | **Tafel slope (mV $dec^{-1}$)** | **Reference** |
|---|---|---|---|
| CoP/$Ni_2$P@HPNCP | 130 | 63.38 | This work |
| CoP/NCNHP | 140 | 53 | 4 |
| CoP-InNC@CNT | 153 | 62 | 16 |
| Ni–Cu–P films | 150 | 69 | 17 |
| $Co_4Ni_1$P NTs | 131 | 54 | 18 |
| Ni-CoP/HPFs | 144 | 52 | 19 |
| CoP/$Ni_2$P | 174 | 78 | 14 |
| CoP NPs | 135 | 65 | 20 |

**Table S4** Comparison of HER of CoP/$Ni_2P$@HPNCP with other reported phosphide-based bifunctional electrocatalysts in 1.0 M PBS.

| Catalysts | Overpotential at 10 mA $cm^{-2}$ (mV) | Tafel slope (mV $dec^{-1}$) | Reference |
|---|---|---|---|
| CoP/$Ni_2P$@HPNCP | 141 | 87.2 | This work |
| CoP-400 | 161 | 81 | 21 |
| V, N-CoP | 146 | 88 | 22 |
| $Ni_2P$@NPCNFs/CC | 185.3 | 230.3 | 23 |
| NiCoP/rGO | 142 | 91 | 24 |
| Ni-Co-P-H (0.5M PBS) | 157 | 84 | 25 |
| $Co_{0.6}Fe_{0.4}P$-1.125 | 140 | 75 | 26 |

**Table S5** EIS fitting parameters from equivalent circuits of all samples during HER process in 0.5 M $H_2SO_4$.

| Samples | $R_S$ /Ω | $CPE_1$ / S $s^{-n}$ | $n_1$/ 0<n<1 | $R_1$ / Ω | $CPE_2$ / S $s^{-n}$ | $n_2$/ 0<n<1 | $R_{ct}$ /Ω |
|---|---|---|---|---|---|---|---|
| CoP/$Ni_2P$@HPNCP | 8.399 | 4.473 E-004 | 0.89 | 0.339 | 2.326 E-003 | 0.57 | 51.0 |
| CoP@NCP | 8.745 | 9.112 E-005 | 0.80 | 0.337 | 7.359 E-004 | 0.60 | 213.5 |
| Co/Ni@HPNCP | 7.816 | 2.645 E-004 | 0.82 | 8.28 | 8.634 E-004 | 0.59 | 9.464 E+003 |
| Co@NCP | 8.062 | 4.635 E-004 | 0.90 | 5.45 | 1.180 E-003 | 0.69 | 1.478 E+004 |

**Table S6** EIS fitting parameters from equivalent circuits of all samples during HER process in 1.0 M PBS.

| **Samples** | **$R_S$ /Ω** | **$CPE_1$ / S $s^{-n}$** | **$n_1$/ 0<n<1** | **$R_1$ / Ω** | **$CPE_2$ / S $s^{-n}$** | **$n_2$/ 0<n<1** | **$R_{ct}$ /Ω** |
|---|---|---|---|---|---|---|---|
| CoP/$Ni_2$P@HPNCP | 13.08 | 3.952 E-005 | 0.54 | 23.02 | 3.420 E-003 | 0.54 | 49.52 |
| CoP@NCP | 12.99 | 3.670 E-003 | 0.59 | 24.56 | 7.666 E-004 | 0.46 | 60.99 |
| Co/Ni@HPNCP | 15.25 | 3.566 E-003 | 0.87 | 53.59 | 1.174 E-003 | 0.55 | 3.876 E+003 |
| Co@NCP | 14.94 | 6.024 E-004 | 0.86 | 69.12 | 5.093 E-003 | 0.52 | 8.879 E+003 |

**Table S7** EIS fitting parameters from equivalent circuits of all samples during OER process in 1.0 M KOH.

| **Samples** | **$R_S$ /Ω** | **$Q_1$ / S $s^{-n}$** | **$n_1$/ 0<n<1** | **$R_1$ / Ω** | **$Q_2$ / S $s^{-n}$** | **$n_2$/ 0<n<1** | **$R_{ct}$ /Ω** |
|---|---|---|---|---|---|---|---|
| CoP/$Ni_2$P@HPNCP | 8.532 | 1.425 E-002 | 0.79 | 18.47 | 8.164 E-004 | 0.54 | 76.07 |
| CoP@NCP | 9.785 | 9.159 E-004 | 0.56 | 13.05 | 9.174 E-003 | 0.79 | 107.5 |
| Co/Ni@HPNCP | 9.453 | 4.317 E-003 | 0.46 | 31.5 | 2.328 E-003 | 0.82 | 593.0 |
| Co@NCP | 9.464 | 9.938 E-005 | 0.77 | 83.31 | 9.728 E-003 | 0.59 | 918.1 |

**References**


1. L. Zhang, X. Ren, X. Guo, Z. Liu, A. M. Asiri, B. Li, L. Chen and X. Sun, *Inorg. Chem.*, 2018, **57**, 548-552.
2. G. Li, J. Yu, W. Yu, L. Yang, X. Zhang, X. Liu, H. Liu and W. Zhou, *Small*, 2020, **16**, e2001980.
3. G. Zhao, K. Rui, S. X. Dou and W. Sun, *Adv. Funct. Mater.*, 2018, **28**, 1803291.
4. Y. Pan, K. A. Sun, S. J. Liu, X. Cao, K. L. Wu, W. C. Cheong, Z. Chen, Y. Wang,

Y. Li, Y. Q. Liu, D. S. Wang, Q. Peng, C. Chen and Y. D. Li, *J. Am. Chem. Soc.*, 2018, **140**, 2610-2618.

5. J. S. Li, L. X. Kong, Z. X. Wu, S. Zhang, X. Y. Yang, J. Q. Sha and G. D. Liu, *Carbon*, 2019, **145**, 694-700.
6. T. T. Liang, Y. D. Liu, P. F. Zhang, C. T. Liu, F. Ma, Q. Y. Yan and Z. F. Dai, *Chem. Eng. J.*, 2020, **395**, 10.
7. H. Liu, J. Guan, S. Yang, Y. Yu, R. Shao, Z. Zhang, M. Dou, F. Wang and Q. Xu, *Adv. Mater.*, 2020, **32**, 2003649.
8. Y. T. Wu, H. Wang, S. Ji, B. G. Pollet, X. Y. Wang and R. F. Wang, *Nano Research*, 2020, **13**, 2098-2105.
9. X. J. Wei, Y. H. Zhang, H. C. He, L. Peng, S. H. Xiao, S. R. Yao and P. Xiao, *Chem. Commun.*, 2019, **55**, 10896-10899.
10. P. X. Ji, H. H. Jin, H. L. Xia, X. Luo, J. K. Zhu, Z. H. Pu and S. C. Mu, *ACS Appl. Mater. Interfaces*, 2020, **12**, 727-733.
11. X. X. Ma, Y. Q. Chang, Z. Zhang and J. L. Tang, *J. Mater. Chem. A*, 2018, **6**, 2100-2106.
12. K. He, T. T. Tsega, X. Liu, J. Zai, X.-H. Li, X. Liu, W. Li, N. Ali and X. Qian, *Angew. Chem. Int. Ed.*, 2019, **58**, 11903-11909.
13. Q. Shi, Q. Liu, Y. Ma, Z. Fang, Z. Liang, G. Shao, B. Tang, W. Y. Yang, L. Qin and X. S. Fang, *Adv. Energy Mater.*, 2020, **10**, 11.
14. J. Zhang, S. Wei, Y. Liu, G. Wang, Y. Cui, A. Dong, S. Xu, J. Lian and Q. Jiang, *J. Mater. Chem. A*, 2019, **7**, 26177-26186.
15. H. P. Feng, L. Tang, G. M. Zeng, J. F. Yu, Y. C. Deng, Y. Y. Zhou, J. J. Wang, C. Y. Feng, T. Luo and B. B. Shao, *Nano Energy*, 2020, **67**, 11.
16. L. L. Chai, Z. Y. Hu, X. Wang, Y. W. Xu, L. J. Zhang, T. T. Li, Y. Hu, J. J. Qian and S. M. Huang, *Adv. Sci.*, 2020, **7**, 10.
17. M. Cao, Z. Xue, J. Niu, J. Qin, M. Sawangphruk, X. Zhang and R. Liu, *ACS Appl. Mater. Interfaces*, 2018, **10**, 35224-35233.
18. L. Yan, L. Cao, P. Dai, X. Gu, D. Liu, L. Li, Y. Wang and X. Zhao, *Adv. Funct. Mater.*, 2017, **27,** 1703455.

19. Y. Pan, K. A. Sun, Y. Lin, X. Cao, Y. S. Cheng, S. J. Liu, L. Y. Zeng, W. C. Cheong, D. Zhao, K. L. Wu, Z. Liu, Y. Q. Liu, D. S. Wang, Q. Peng, C. Chen and Y. D. Li, *Nano Energy*, 2019, **56**, 411-419.
20. Y. Liu, Y. Zhu, J. Shen, J. Huang, X. Yang and C. Li, *Nanoscale*, 2018, **10**, 2603-2612.
21. H. Li, X. Zhao, H. Liu, S. Chen, X. Yang, C. Lv, H. Zhang, X. She and D. Yang, *Small*, 2018, **14**.
22. W. Zhang, Y. Sun, Q. Liu, J. Guo and X. Zhang, *J. Alloys Comp.*, 2019, **791**, 1070-1078.
23. M.-Q. Wang, C. Ye, H. Liu, M. Xu and S.-J. Bao, *Angew. Chem. Int. Ed.*, 2018, **57**, 1963-1967.
24. J. Li, M. Yan, X. Zhou, Z.-Q. Huang, Z. Xia, C.-R. Chang, Y. Ma and Y. Qu, *Adv. Funct. Mater.*, 2016, **26**, 6785-6796.
25. X. Liu, S. Deng, D. Xiao, M. Gong, J. Liang, T. Zhao, T. Shen and D. Wang, *ACS Appl. Mater. Interfaces*, 2019, **11**, 42233-42242.
26. Y. B. Lian, H. Sun, X. B. Wang, P. W. Qi, Q. Q. Mu, Y. J. Chen, J. Ye, X. H. Zhao, Z. Deng and Y. Peng, *Chem. Sci.*, 2019, **10**, 464-474.